# MO Analysis of the Fluxional Behavior of $M(\eta^3\text{-}S_2CPMe_3)(CO)_2(PMe_3)_2$ (M = Mo, W) Complexes

**Agustín Galindo*,† and Carlo Mealli*,‡**

Departamento de Química Inorgánica, Universidad de Sevilla, Aptdo 553, 41071 Sevilla, Spain, and ISSECC-CNR, Via J. Nardi 39, 50132 Firenze, Italy

*Received July 27, 1995*

Trialkylphosphinedithiocarboxylato ligands, $S_2CPR_3$, show a great variety of coordination modes to a transition metal atom. In particular, the $\eta^3$-(*S, S′, C*) coordination has attracted considerable interest in recent years as it has been structurally characterized in a number of mononuclear[1] and binuclear[2] complexes.

Recently, Carmona et al. have reported the synthesis of $M(S_2CPMe_3)(CO)_2(PMe_3)_2$ (M = Mo, **1a**;[3] W, **1b**[4]) complexes that contain the $S_2CPMe_3$ ligand $\eta^3$-bonded to the metal, according to the X-ray crystal structure of **1b**. These compounds show fluxional behavior in solution, and as an example, the variable-temperature $^{31}P\{^1H\}$ NMR spectrum for **1b** is displayed in Figure 1. At 20 °C it consists of a triplet at $\delta$ 31.7 ($S_2CPMe_3$, $^3J_{PP} = 4.5$ Hz) and a very broad signal at about $\delta$ −30 ($2PMe_3$), the latter converting into a somewhat broad singlet upon heating the sample to 80 °C. This signal separates into two resonances at temperatures below −20 °C, and at −70 °C a doublet ($\delta$ −16.2) and a doublet of doublets ($\delta$ −38.6) are observed.

This note describes a theoretical study directed towards the understanding of this fluxional process and the explanation of the dynamic NMR spectra. For this purpose, EHMO calculations, comprising the analysis of the relevant fragment molecular orbital (FMO) interactions, have been performed.[5]

As a starting point for the MO description of the $\eta^3$-coordination of the $S_2CPR_3$ ligand, the simplest butterfly $MoH_4^{4-}$ fragment (derived from an octahedron upon removal of two *cis* ligands[6]) was used. A simplified interaction diagram is presented in Figure 2. On the right side, the most significant metal FMOs consist of a high lying $\sigma$ hybrid, a $d_\pi$ hybrid, and the three "$t_{2g}$" members.[16] On the left side, the FMOs of the $S_2CPH_3$ ligand consist of the three combinations of the $\pi$-$S_2C$ system (bonding $\pi$-$S_2C$, nonbonding $\pi^n$-$S_2C$, and antibonding $\pi^*$-$S_2C$). Figure 2 highlights the major interactions: the donations from the filled $\pi$-$S_2C$ and $\pi^n$-$S_2C$ FMOs into the metal $\sigma$ and $d_\pi$ hybrids, as well as the back-donation from the metal into $\pi^*$-$S_2C$. As also shown by the 3D drawing of the MO 2S, $x^2 - y^2$ mixes in *xz* orbital character to better saturate the residual electrophilicity at the central C atom of the dithioacid ligand.[7]

The study of the Mo−$S_2CPH_3$ linkage can then be extended to the more realistic model compounds in which two $PH_3$ and two CO ligands replace the hydrides while still maintaining the $C_{2v}$ symmetry. In these initial models, the two CO ligands alternatively occupy either the two axial or the two equatorial positions. Because of their strong $\pi$ acceptor character, equatorial carbonyls stabilize all of the $t_{2g}$ orbitals at different extents ($x^2 - y^2 > yz > xz$, by 1.2, 0.6, and 0.5 eV, respectively). In this case, the large energy gap disfavors the back-donation into $\pi^*$-$S_2C$, which involves both the $x^2 - y^2$ and *xz* orbitals. The situation is somewhat different with two *trans*-axial CO ligands which leave the $x^2 - y^2$ orbital unperturbed (*ca.* 0.8 eV above *xz* and *yz*). Also, the angular $\alpha$ and $\beta$ distortions, indicated in **I** ($90° < \alpha < 110°$; $180° > \beta > 150°$), are in either case important in determining the strength of the metal back-donation to the $S_2C$ carbon atom. In particular, the decrease of $\beta$ from 180 to 150° introduces ligand to metal $\sigma^*$ character in the *xz* orbital.[8] The ensuing destabilization determines a larger contribution of the latter orbital to the back-donation into $\pi^*$-$S_2C$. In summary, the relative disposition of the ligands as well as the angular deformations appear to be governing factors for the fluxional behavior of the $\eta^3$ complex now under consideration.[17]

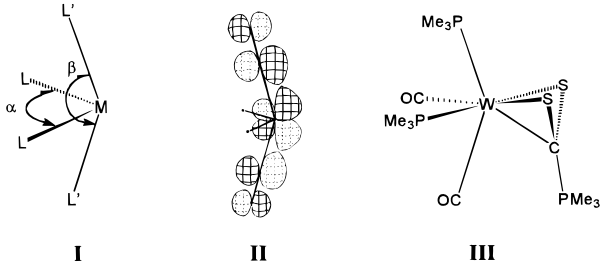


**I** **II** **III**

Quantitatively, in the presence of two equatorial COs, the combined deformation of type **I** destabilizes the *xz* orbital by *ca.* 1 eV (eventually to become the isolated HOMO of the fragment) and the whole $ML_4$ fragment loses *ca.* 1.7 eV. In contrast, the corresponding fragment with two axial COs has a total energy that is initially *ca.* 0.7 eV higher (recall that $x^2 - y^2$ is not stabilized by the COs), but the deformation **I** does not induce a comparably large destabilization. In this latter case, the *xz* orbital rises in energy (due to the acquired Mo−CO $\sigma^*$ character) but not as steeply as before due to the residual stabilization provided by the two $\pi^*_{CO}$ levels (see **II**). Ultimately, since the $x^2 - y^2$ orbital remains the HOMO of the fragment, closest to the $\pi^*$-$S_2C$ level, the reciprocal interaction between the two never becomes as efficient as if there were a larger involvement of *xz*. Certainly, this could be better achieved in presence of two equatorial COs, but the overall energy cost of the fragment deformation is too high.

Although the analysis is complicated by the lack of symmetry, the best $\eta^3$ interaction (also corresponding to the minimal total energy) occurs with the ligand arrangement found in the crystal structure of **1b** (see **III**). Evidently, the factors which disfavor either two equatorial or two axial COs, are slackened. Since the energy of neither the *xz* nor the $x^2 - y^2$ orbital is too

† Universidad de Sevilla
‡ ISSECC-CNR.

(1) Carmona, E.; Gutiérrez-Puebla, E.; Monge, A.; Pérez, P.; Sánchez, L. *Inorg. Chem.* **1989**, *28*, 2120.
(2) See for example : (a) Miguel, D.; Pérez-Martínez, J. A.; Riera, V.; García-Granda, S. *Organometallics* **1994**, *13*, 4667. (b) Miguel, D.; Pérez-Martínez, J. A.; Riera, V.; García-Granda, S. *Organometallics* **1994**, *13*, 1336. (c) Miguel, D.; Riera, V.; Miguel, J. A.; Gómez, M.; Soláns, X. *Organometallics* **1991**, *10*, 1683 and references therein.
(3) Carmona, E.; Galindo, A.; Monge, A.; Muñoz, M. A.; Poveda, M. L.; Ruiz, C. *Inorg. Chem.* **1990**, *29*, 5074.
(4) Galindo, A.; Gutiérrez-Puebla, E.; Monge,A.; Pastor, A.; Pizzano, A.; Ruiz, C.; Sánchez, L.; Carmona, E. *Inorg. Chem.* **1993**, *32*, 5569.
(5) (a) Hoffmann, R. *J. Chem. Phys.* **1963**, *39*, 1397. (b) Hoffmann, R.; Lipscomb, W. N. *J. Chem. Phys.* **1962**, *36*, 2179 and 2872.
(6) Albright, T. A.; Burdett, J. K.; Whangbo, M.-H. *Orbital Interactions in Chemistry*, Wiley: New York, 1985.
(7) For chemical reactivity confirming this electrophilic character see: (a) Bianchini, C.; Meli, A.; Dapporto, P.; Tofanari, T.; Zanello, P. *Inorg. Chem.* **1987**, *26*, 3677. (b) Bianchini, C.; Mealli, C.; Meli, A.; Scapacci, G. *Organometallics* **1983**, *2*, 141. (c) Bianchini, C.; Meli, A.; Orlandini, A. *Inorg. Chem.* **1982**, *21*, 4161.
(8) Elian, M.; Hoffmann, R. *Inorg.Chem.* **1975**, *14*, 1058.
(9) Galindo, A.; Mealli, C.; Cuyas, J.; Miguel, D.; Riera, V.; Pérez-Martínez, J.; Bois, C.; Jeannin, Y. Submitted for publication in *Organometallics*.

0020-1669/96/1335-2406$12.00/0 

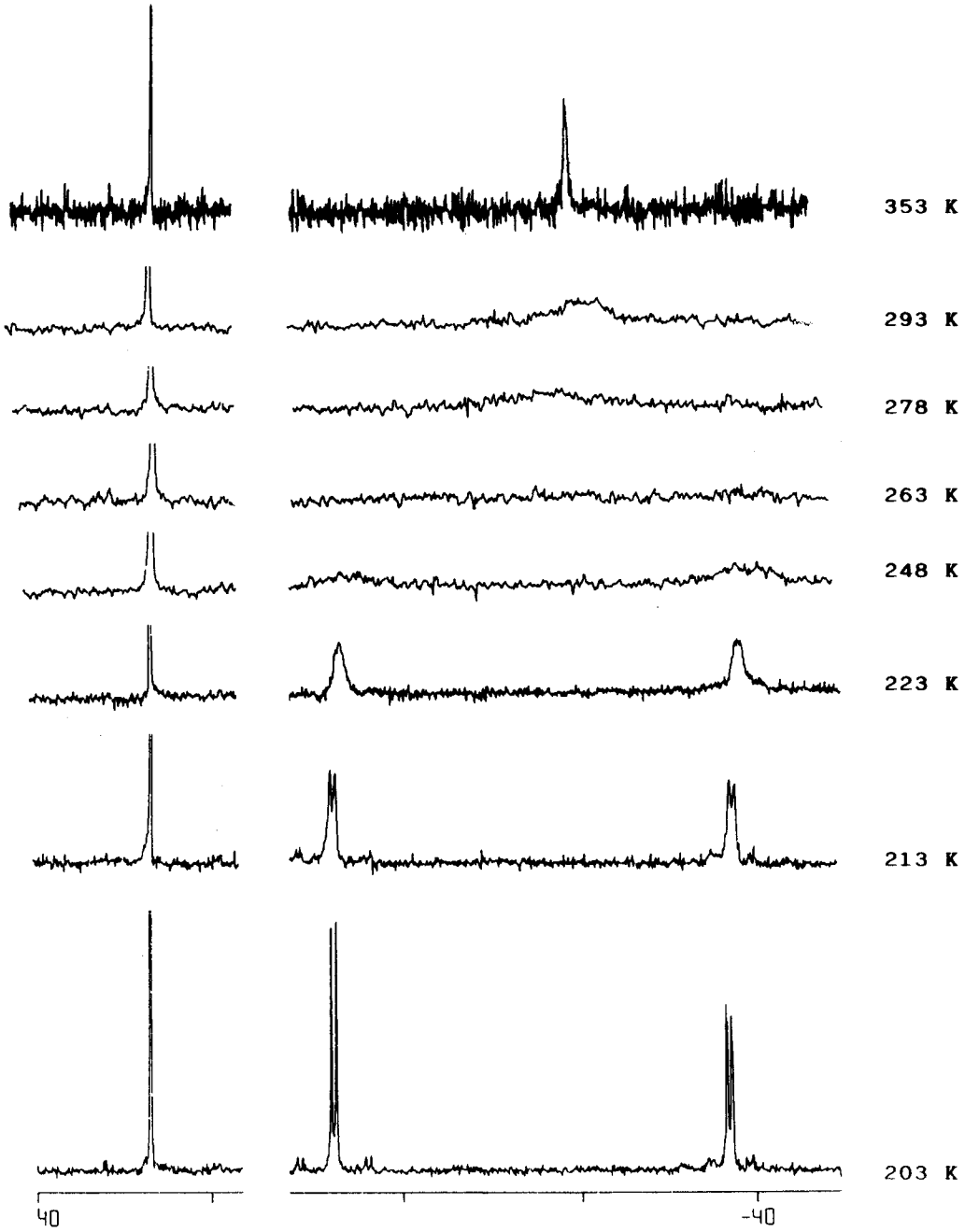


**Figure 1.** Variable temperature $^{31}P\{^{1}H\}$ NMR spectra of **1b** in toluene-$d_8$.

depressed, and since they remain close to each other so as to mix constructively, they jointly support the Mo−C bond of the $\eta^3$ conformation. The drawings of the bonding MOs containing a mixture of the xz and $x^2 - y^2$ orbitals are shown in order in **IV** and **V**. They represent the HOMO and a sligthly lower energy filled MO, respectively.

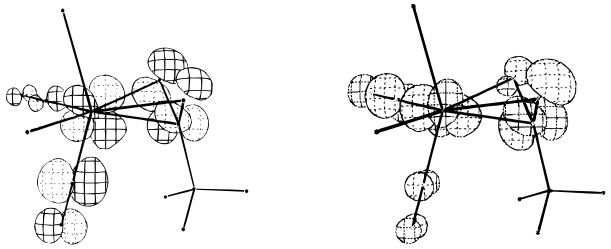

**IV** **V**

It is noteworthy that a calculation in which the C−P vector of $S_2CPH_3$ eclipses the axial $PH_3$ in place of the *trans* CO ligand shows that the conformation **III** is favored by *ca.* 1 eV.[10] Overlap arguments do easily account for the result. Thus, the fluxional behavior was assumed to be associated with a restricted intramolecular process ($^{31}P-^{31}P$ coupling is mantained in the fast exchange regime). The $S_2CPMe_3$ fragment undergoes propeller rotation (see **VI**) between the two Mo−CO bonds in a concerted Berry-pseudorotational process on the $Mo(CO)_2(PMe_3)_2$ fragment (see **VII**). Viewed down the metal−ligand rotation axis (dashed line in **VI**), the C−P vector of the dithioacid ligand is seen to move between the two Mo−CO vectors.

The significant MO aspects of the pseudorotation can be monitored by a Walsh type diagram (Figure 3). Step 3 corresponds to a square pyamidal geometry ($\alpha = \beta = 130°$) in which the $S_2CPMe_3$ ligand occupies the apical position and the C−P vector bisects the angle formed by the two cisoid CO

(10) For similar conformational preferences see for example: Chardon, C.; Eisenstein, O.; Johnson, T.; Caulton, K. *New. J. Chem.* **1992**, *16*, 781 and references therein.

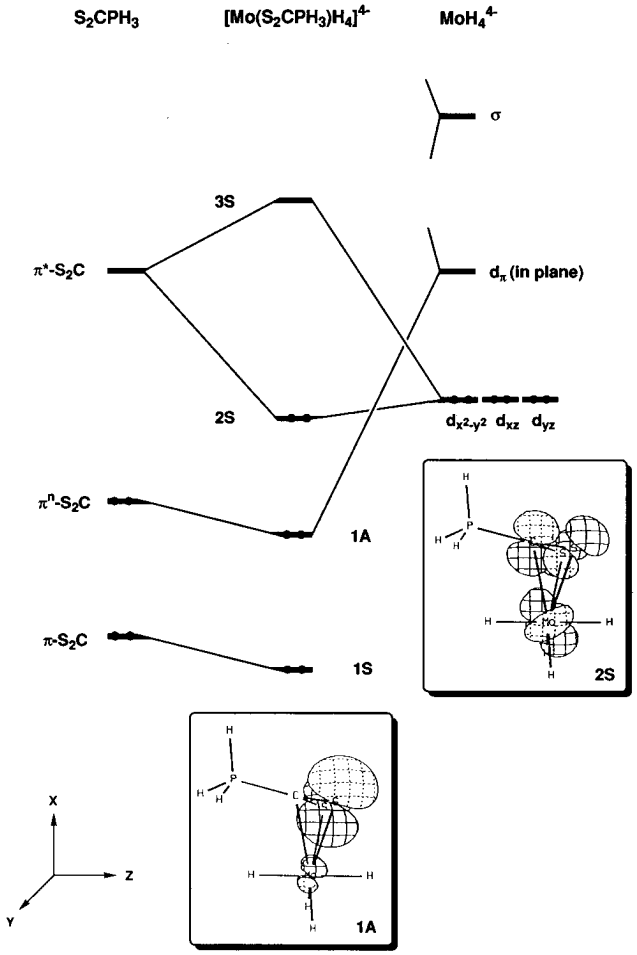


**Figure 2.** Simplified interaction diagram for the model compound [Mo($\eta^3$-$S_2CPH_3$)$H_4$]$^{4-}$.

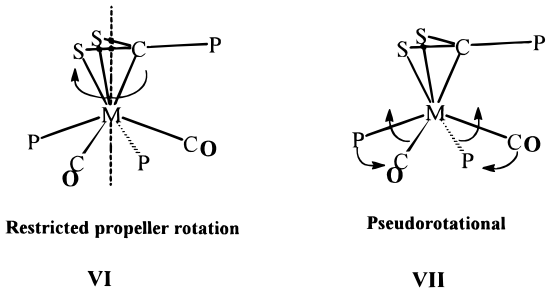


**VI** **VII**

ligands. This intermediate has $C_s$ symmetry. Steps 1 and 5 are equivalent eclipsed conformations with no symmetry ($C_1$).

Only the six higher filled MOs are shown in Figure 3. It appears that the levels 1 and 6 are responsible for the calculated energy barrier of *ca.* 1 eV. With reference to the oversimplified model of Figure 2, the lowest MO (1) is primarily bonding between the $\pi^n$-$S_2C$ FMO and the metal $d_\pi$ hybrid, MO 1A, while the 1S level lies at lower energy and it is not shown. The highest MO (6) corresponds to the back-bonding MO **IV** (MO 2S in Figure 2). All of the bonding interactions are evidently maximized when the $S_2C$ plane is bisected from one P−Mo−CO plane. The remaining frontier MOs (2−5) are less unaffected. From higher to lower energy, these correspond to two $t_{2g}$ levels (*xz*, *yz*) and to in-phase and out-of-phase combinations of sulfur lone pairs in the $S_2C$ plane ($\sigma^n$-$S_2C$ (i.p.) and $\sigma^n$-$S_2C$ (o.o.p.), respectively) not previously pointed out. One of the latter two levels is schematically drawn in Figure 3.

The experimental[11] activation parameters obtained by band shape analysis of the $^{31}P\{^1H\}$ NMR spectra of complex **1b** are

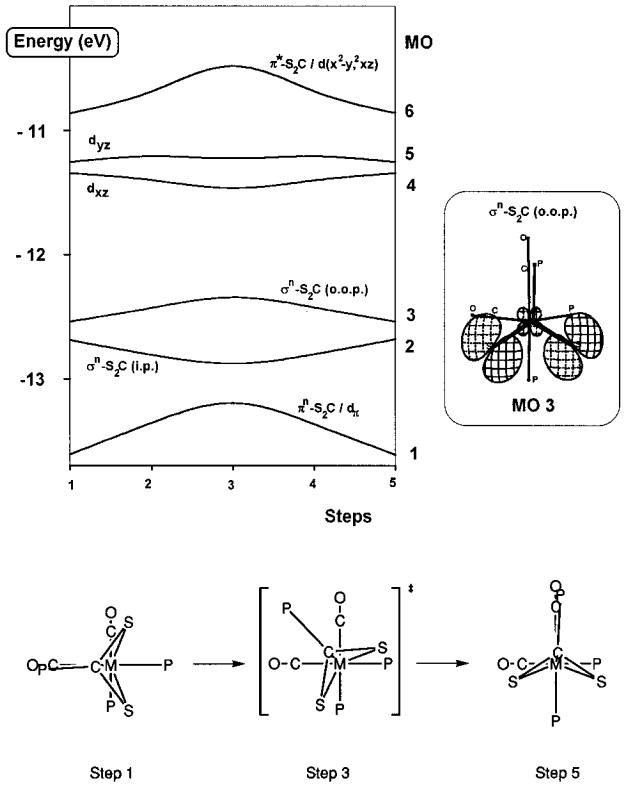


**Figure 3.** Walsh diagram that monitors the evolution of the frontier MO for the fluxional propeller rotation mechanism. All of the levels are populated and their original nature is described with reference to the MOs of the simplified model of Figure 2.

$\Delta H^{\ddagger} = 39.2$ kJ mol$^{-1}$ and $\Delta S^{\ddagger} = -30$ J K$^{-1}$ mol$^{-1}$. This energetic barrier (*ca.* 0.5 eV) is confirmed by calculation although the calculated value of *ca.* 1 eV is significantly higher. A tentative explanation for the higher energetics is likely to be found in the well-known overestimation of the repulsion between the in-plane 1,3 sulfur lone pairs (level 3 in Figure 3) by the EHMO method.[13] Even though we observed that the barrier can be somewhat lowered by opening the S−C−S angle more than its experimental value (117°), no attempt was made to optimize the overall geometry.

**Acknowledgment.** A.G. is grateful to the Ministerio de Educación y Ciencia (Spain) for financing his stay at the ISSECC. The authors also thank the EC for financial support under Contract No. CHRX-CT93-0147.

## Appendix

The extended Hückel parameters were taken from ref 14. The bond distances and angles used in the extended Hückel calculations have been taken from the X-ray results.[1,4] The MO drawings have been obtained by using the CACAO program.[15]

IC9509138

(11) Rate costants for the proposed propeller rotation mechanism were calculated by using DNMR.[12] An iterative nonlinear least-squares regression analysis to obtain the best fit of the experimental spectra was used. Activation parameters were obtained from the slope and intercept of an Eyring plot.

(12) Stephenson, D. S.; Binsch, G. *J. Magn. Reson.* **1978**, *32*, 145.
(13) Mealli, C.; Hofmann, R.; Stockis, A. *Inorg. Chem.* **1984**, *23*, 56.
(14) Alvarez, S. *Tables of Parameters for Extended Hückel Calculations*; Departamento de Química Inorgánica, Universidad de Barcelona: Barcelona, Spain, 1989.
(15) Mealli, C.; Proserpio, D. M. *J. Chem. Educ.* **1990**, *67*, 399.
(16) Given the exclusive $\sigma$ donor capabilities of the hydride ligands, the degeneracy of the three "$t_{2g}$" levels is preserved at this geometry.
(17) The same factors have been also found crucial in determining the well-known dichotomy between $\eta^2$ and $\eta^3$ complexes of dithiocarboxylate ligands.[9]